ISSN (Print) 1226-1750
ISSN (Online) 2233-6656
Journal of Magnetics 22(4), 563-569 (2017) https://doi.org/10.4283/JMAG.2017.22.4.563

In-situ Observation of Domain Wall Motion in Electroplated Ni80-Fe20 Thin Film by Lorentz TEM and DPC Imaging

Su Jin Lee[1], Hyo-Jong Lee[1], Kyung Song[2], Si-Young Choi[2], and Hyun Soon Park[3]*

[1]*Department of Materials Science and Engineering, Dong-A University, Busan 49315, Republic of Korea*
[2]*Mateirals Modeling and Characterization Department, Korea Institute of Materials Science (KIMS), Changwon 51508, Republic of Korea*
[3]*Department of Materials Science and Engineering, Inha University, Incheon 22212, Republic of Korea*

(Received 8 August 2017, Received in final form 28 September 2017, Accepted 16 October 2017)

***In-situ* observations of magnetic domain wall motion in a Ni80-Fe20 thin film electroplated on a Cu film were performed by Lorentz TEM. Detailed magnetization distribution was investigated by differential phase contrast microscopy. The magnetic properties of the coercivity and saturation magnetic flux density were measured to be 6.5 Oe and 1.56 T, respectively. The diffraction ring pattern showed the Ni_3Fe FCC structure with nanocrystalline nature (grain size 29 nm) and texture indicating the preferential orientation. We measured the domain width of 1.9 μm and found the fluctuation of magnetization direction coupled with two vortices. With the in-plane and out-of-plane magnetic fields applied, domain wall motions were *in-situ* observed and discussed.**

Keywords : permalloy, electroplating, magnetic domain, TEM, Lorentz microscopy, STEM

1. Introduction

Permalloy (Ni80-Fe20wt.%), a representative soft magnetic material, has high magnetic permeability and low coercivity (H_c). The permalloy thin films are used for various electromagnetic devices such as magnetic recording heads, micro-actuator and magnetic shielding [1-3]. Recently, the soft magnetic materials require large saturation magnetic flux density (B_s) and low coercivity due to increasing requirement of miniaturization for the electromagnetic devices [4]. To meet these properties of the devices, an electroplating as well as the sputtering is an alternative method to fabricate thin films [2, 5]. Also, the electroplating enables us to make high purity films with short time in process, resulting in the low hysteresis loss [6, 7].

The magnetic properties of permalloy thin film are affected by both microstructures and magnetic domains [1, 4, 8]. Moreover, its electrical resistivity can vary as much as 5 % depending on the strength and the direction of applied magnetic field. Soft magnetic alloys with nanocrystallinity have been thus developed because of their excellent magnetic properties such as high B_s, low H_c, and low core loss [9]. Considering a low H_c, the magnetocrystalline anisotropy is averaged out because of the exchange coupling of randomly oriented nanograins [10]. The H_c depends on the grain size (g), which is proportional to g^6 below 50 nm but g^{-1} above 50 nm [6, 8, 11]. To the predominant factor affecting H_c and core loss, it is necessary to observe the magnetic microstructure as well as domain wall motion. Therefore, the motivation in this study is to study the correlation between magnetic microstructure and dynamics of domain walls with applied magnetic field [1, 12].

In-situ observation of magnetic domains in space and time can be studied by various microscopy techniques, *i.e.*, magnetic force microscopy, magneto-optical Kerr microscopy, scanning transmission X-ray microscopy, Lorentz transmission electron microscopy (TEM) and differential phase contrast (DPC) microscopy [4, 13]. In this study, the Fresnel method of Lorentz microscopy and DPC microscopy were utilized to *in-situ* observe the domain wall motion as well as magnetic microstructure in electroplated Ni80-Fe20 thin film. Furthermore, the relationship between the theoretical and measured values of domain width was briefly discussed.

*Corresponding author: Tel: +82-32-860-7533
Fax: +82-32-862-5546, e-mail: hsparkinha@inha.ac.kr

2. Experimental Procedure

Schematic illustration of electroplating on Cu film at 323 K is shown in Fig. 1(a). The permalloy thin film with composition of Ni80-Fe20 wt.% was obtained in electrolyte including about 8.5 g of iron chloride tetrahydrate ($FeCl_2 \cdot 4H_2O$) in Fig. 1(b). In Fig. 1(c) the thicknesses of Ni80-Fe20 and Cu thin films were measured as 3 μm and 8 μm, respectively. The hysteresis loop of Ni80-Fe20 thin film was measured using a magnetic property measurement system (MPMS-7). The magnetic field (H) at 300 K shown in Fig. 1(c) was applied perpendicular to the Ni80-Fe20 film plate which size was approximately 5 mm × 3 mm × 3 μm. We need to control the thickness and shape of TEM specimen because the soft magnetic materials have quite low magnetic anisotropy, which may affect the magnetic domain structure. Thus, TEM thin foil specimen was prepared by dual beam focused ion beam with lift-off method (FIB, Nova 200 at NanoFab.). The size of TEM specimen was controlled to be approximately 10 μm × 9 μm × 84 nm as shown in Figs. 1(c)-(f). Electron energy loss spectroscopy (EELS) measurement was utilized to investigate the thickness distribution of TEM specimen.

Microstructures, *i.e.*, g distribution and texture, were observed by dark-field TEM and diffraction patterns. DPC imaging was performed by STEM (JEM 2100F at KIMS). The DPC images were obtained by segmented detector (8 segments) which was utilized to detect the Lorentz defection of the electron beam [14]. *In-situ* observations of magnetic domain wall motion were performed by Lorentz microscopy using a JEM-2100F HR (NanoFab.) and JEM 2100 (KIMS). The magnetic domain walls are observed to be black lines or white lines because of the divergent or convergent of electrons in the defocus condition of under and over focus [13, 15]. In order to observe the magnetic domains, the experiment was conducted in low magnification mode switching off the objective lens. The residual magnetic field (H_r) at specimen position was estimated to be about 150 Oe [14]. To apply magnetic field to the film plane, we utilized the in-plane component of applied magnetic field (out of plane H_o = 360 Oe) by tilting the TEM specimen. The magnitude of the field applied was estimated using the equation of $H_{//} = H_o \sin\theta$ [13].

3. Results and Discussion

Figure 2(a) shows a bright-field image obtained from the cross section of electroplated Ni80-Fe20 thin film on Cu film prepared by FIB. Selected area diffraction pattern in Ni80-Fe20 thin film (Fig. 2(b)) shows the debye-scherrer rings that are generally formed by numerous

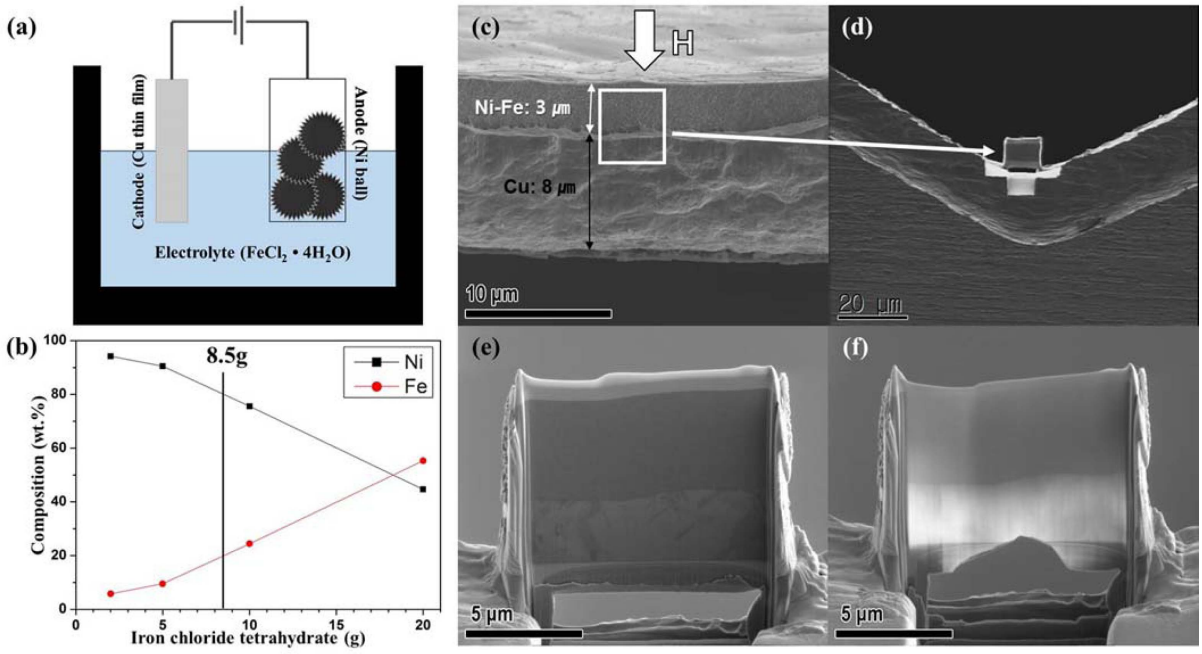

Fig. 1. (Color online) (a) Schematic illustration of electroplating for a Ni80-Fe20 thin film. (b) Ni and Fe composition variation depending on the amount of iron chloride tetrahydrate. (c)-(f) Scanning electron microscope images of the TEM thin foil specimen prepared by FIB. (c) White arrow indicating the direction of magnetic field applied (H) in MPMS. (d) TEM thin foil specimen corresponding to a rectangular region of (c). (e) and (f) were taken under the process of milling specimen below 100 nm.

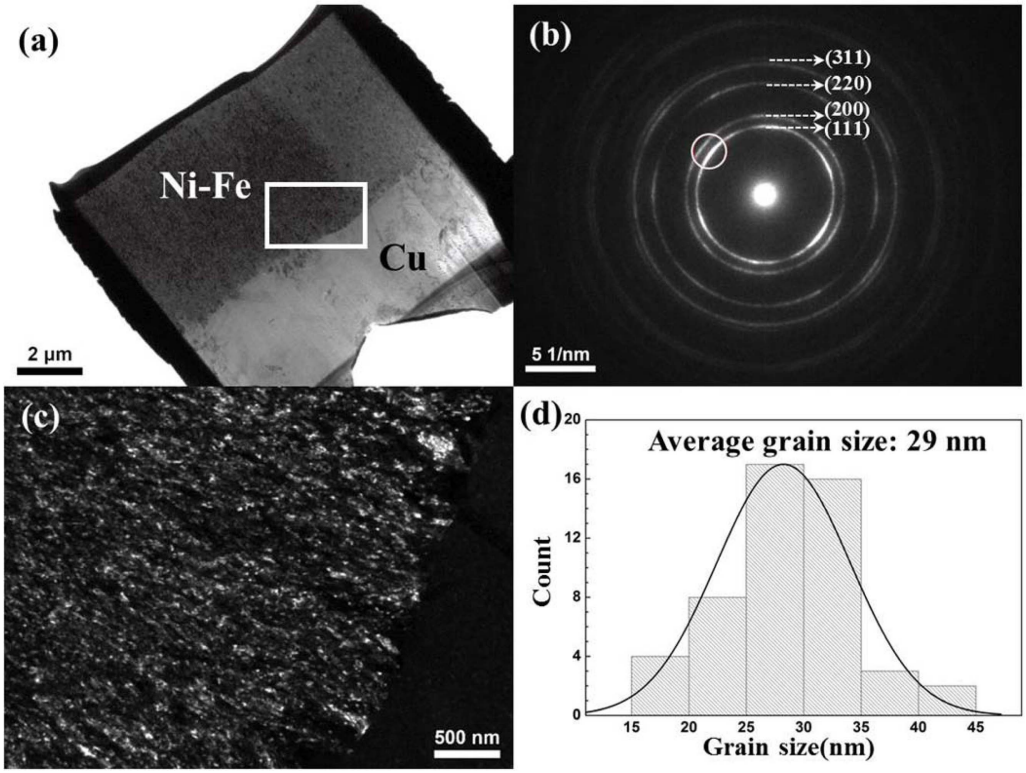

Fig. 2. (a) TEM bright-field image showing a cross section of electroplated Ni80-Fe20 thin film on Cu film prepared by FIB. (b) Selected area electron diffraction pattern of Ni80-Fe20 thin film representing Debye-Scherrer rings. (c) Dark-field image obtained by selecting the (111) and (002) of (b). (d) Grain size distribution of the Ni80-Fe20 film with the average 29 ± 1 nm.

diffraction spots from a large number of randomly oriented nanocrystalline material. Representative planes of Ni_3Fe FCC structure were indicated in Fig. 2(b). Figure 2(c) displays a dark-field image obtained by selecting the (111) and (200) indicated in Fig. 2(b), corresponding to the rectangular region of Fig. 2(a). It is interesting to note that there exist the features of texture in debye-scherrer rings, indicating that the crystallinity represents the preferential orientation. The texture shown in (111) of Fig. 2(b) was affected by the Cu substrate film with a preferential orientation of (111). In order to confirm the *g*, we measured a total of 50 grains in the dark-field image of Fig. 2(d). The average *g* of Ni80-Fe20 film was measured to be 29 ± 1 nm.

Elemental mapping images are shown in Ni80-Fe20 thin film on Cu film of Fig. 3, which was obtained by energy dispersive X-ray spectroscopy. The compositions of Ni and Fe were estimated as about 83 wt.% and 17 wt.%, respectively, which is reasonable composition for us to consider as a permalloy.

Figure 4 and Table 1 show the hysteresis loop and measured magnetic properties of electroplated Ni80-Fe20 thin film by MPMS, respectively. The magnetic field was applied perpendicular to the Ni80-Fe20 film plane as

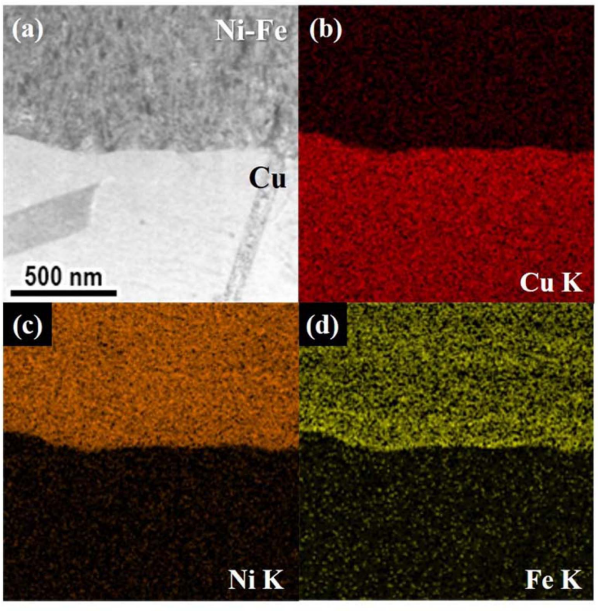

Fig. 3. (Color online) (a)-(d) EDS elemental mapping image showing elementary distribution (Cu, Ni, Fe).

shown in Fig. 1(c). The *B-H* curve indicates typical soft magnetic materials, where the H_c, B_s and remanent flux density (B_r) were measured to be 6.5 Oe, 1.56 T and 0.01

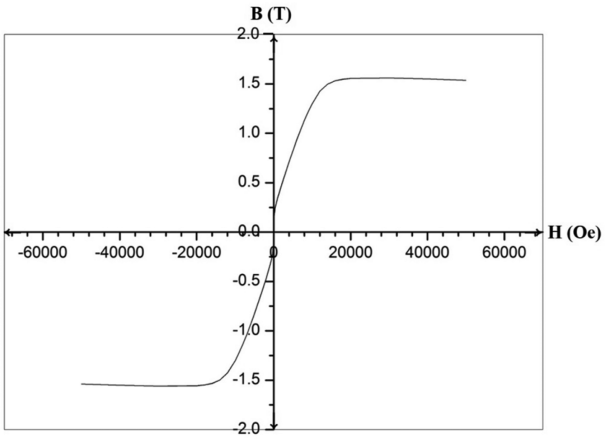

Fig. 4. Hysteresis loop of the Ni80-Fe20 thin film measured by MPMS. The magnetic field (*H*) was applied perpendicularly to the film plane as mentioned above Fig. 1(c).

Table 1. Magnetic properties of Ni80-Fe20 thin film measured by MPMS.

	B_s (T)	B_r (T)	H_c (Oe)
Ni80-Fe20 film	1.56	0.01	6.5

T, respectively. It is known that the B_s and H_c in commercially used permalloy are approximately 0.75 T (~100 μm) and 2.5 Oe (for 13 nm grain size), respectively [16-18]. We consider that our experimental values, *i.e.*, B_s (1.56 T) and H_c (5.6 Oe), are attributed to nanocrystalline nature; that is, H_c is proportional to g^6 below 50 nm.

Figures 5(a) and (c) show Lorentz microscope images of Ni80-Fe20 film without applied magnetic field, which was taken under the defocused conditions of ± 4 μm. White arrow and black double-headed arrow indicate the magnetic domain wall (*DW*) and domain width (*D*), respectively. Peculiar magnetic *DW*s indicated by yellow arrows in Fig. 5(c) were observed, which penetrated the vertical *DW*s. In order to understand detailed magnetization directions, we used quantitative phase technology (QPt) simulation based on transport of intensity equation (TIE) [19, 20]. The phase distribution image in Fig. 5(d) was obtained from three images (Figs. 5(a)-(c)). The color vector map reconstructed from phase image shows the detailed magnetization direction as indicated by white arrows in Figs. 5(e) and (f). The *DW*s were found to undergo an angular displacement of 90° and 180° as well as low-angle observed inside large 180° domains. It is considered that in low-angle *DW*s the fluctuations of magnetization direction reflect the randomly oriented nanocrystalline nature [13].

Further detailed magnetization distribution was studied by DPC images in Fig. 6. Figures 6(a) and (b) show horizontal and vertical DPC components images where black and white contrast correspond to the magnetization direction indicated by the top-left corners. As shown in magnetic induction maps of Figs. 6(c) and (d), the

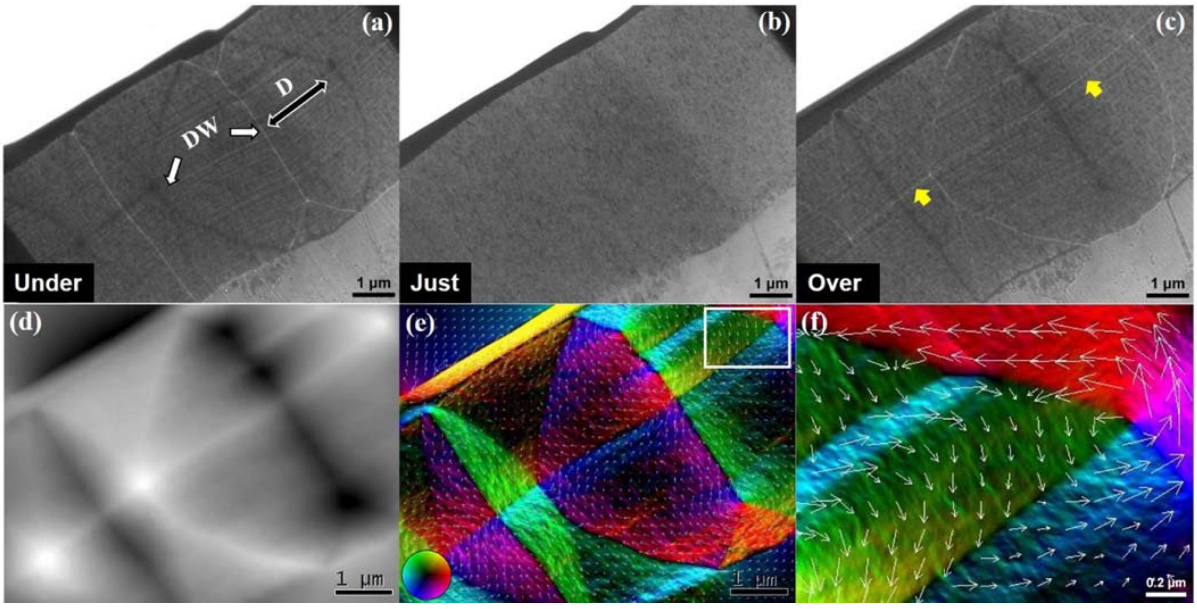

Fig. 5. (Color online) (a) and (c) Lorentz microscope images of the Ni80-Fe20 thin film without applied magnetic field. (b) Just focus (in-focus) image. Defocused values were around ± 4 μm. White and black double-headed arrow in (a) indicate the magnetic domain wall (*DW*) and domain width (*D*), respectively. Yellow arrows indicate the *DW*s penetrating the vertical *DW*s. (d) and (e) Phase distribution image and color vector map, respectively. (f) Magnified image obtained from a rectangular region in inset of (e).

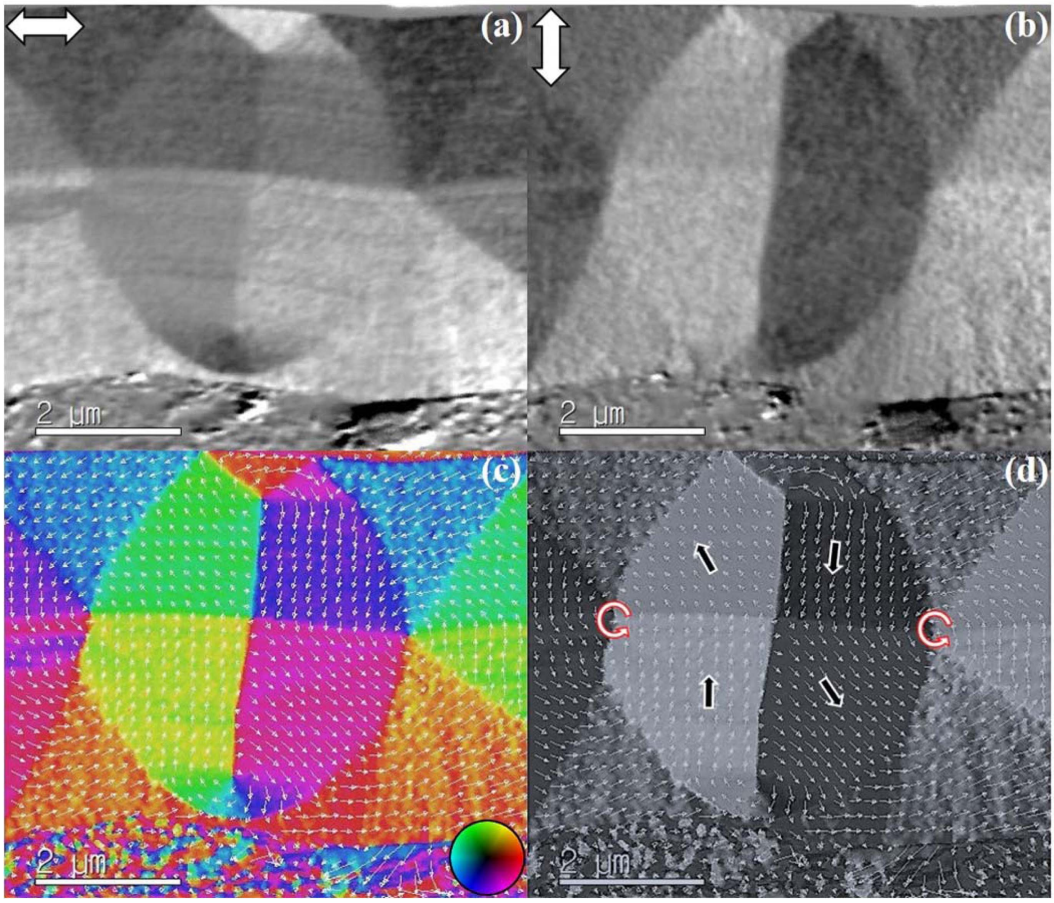

Fig. 6. (Color online) (a) and (b) Horizontal and vertical DPC component images of the Ni80-Fe20 thin film, respectively. (c) and (d) DPC color map showing the distribution of the magnetization direction without applied magnetic field.

distribution of the magnetization direction is more easily understood. The peculiar magnetic *DW*s as mentioned in Fig. 5(c) were found to be attributed to the magnetization distribution like zigzag pattern as shown in Fig. 6(d); that is, two vortices with anticlockwise magnetization direction mainly contribute the formation of *DW*s.

Magnetic domain width (D) was measured as shown in Table 2. The relationship between D and magnetic anisotropy constant (K_u) is

$$D = \sqrt{2\varepsilon_t t / K_u}. \quad (1)$$

Here ε_t and t are the domain-wall energy per unit area and electroplated thickness of Ni80-Fe20 thin film, respectively [21]. The theoretical D in our sample (3 μm thickness) was calculated to be 2.6 μm given from the magnetic parameters of both ε_t (0.22 erg/cm^2) and K_u (2×10^3 erg/cm^3), by using the parameters reported in reference [22, 23]. We measured the averaged D of Ni80-Fe20 as 1.9 μm as shown in Fig. 5(a). This slight discrepancy may due to the different sample thickness and/or grain size.

Figure 7 shows Lorentz microscope images with the in-plane fields ($H_{//}$) applied by tilting the specimen. Black arrows and white arrow indicate the directions of magnetization and $H_{//}$, respectively. Figure 7(a) was obtained under the residual out-of-field (H_o) of about 360 Oe. Sample tilting angle was indicated in insets of the Figs. 7(b)-(f), where the in-plane field was calculated by $H_{//}$=

Table 2. Magnetic domain width (D) and magnetic parameters (domain-wall energy per unit area ε_t, magnetic anisotropy K_u) and thickness (t) of Ni80-Fe20 thin film. The theoretical D for the thickness of 3 μm was calculated as 2.6 μm. The D of 2.6 μm was given from the theoretical value of both ε_t = 0.22 and $K_u = 2 \times 10^3$. We directly measured D of Ni80-Fe20 film as 1.9 μm.

	ε_t (erg/cm^2)	K_u (erg/cm^3)	t (μm)	D (μm)
Theoretical value	0.22 [a]	2×10^3 [b]	3	2.6
Measured value	-	-	Avg. 3	Avg. 1.9

[a]Ref [22]
[b]Ref [23]

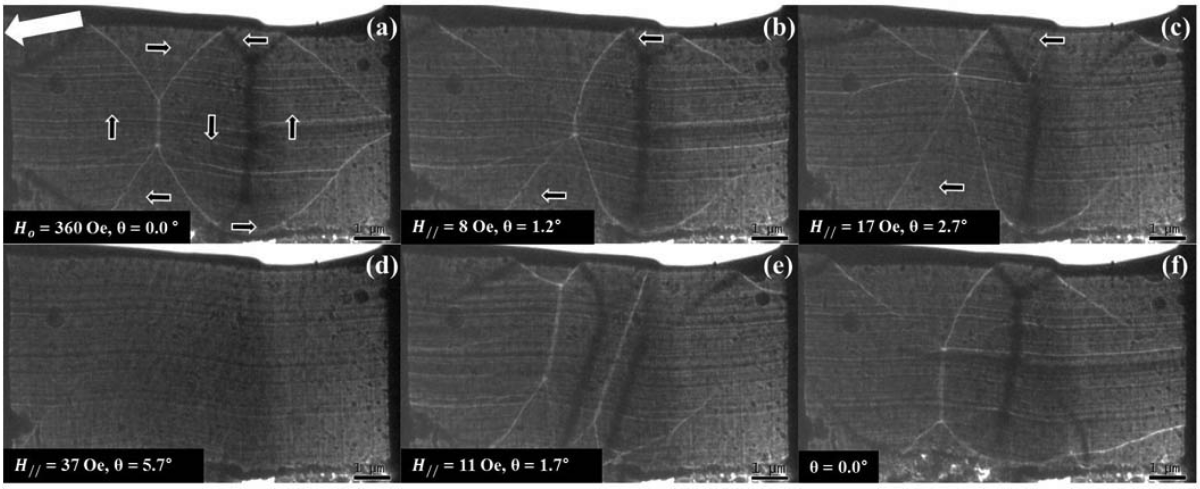

Fig. 7. Lorentz microscope images of Ni80-Fe20 thin film with applied the magnetic field to the in-plane ($H_{//}$). Black arrows and white arrow indicate the directions of magnetization and $H_{//}$, respectively.

$H_o \sin\theta$. With the changes in in-plane fields, the magnetic domains with magnetization direction parallel to the applied film plane increased as shown in Figs. 7(b) and (c). Under the condition of 37 Oe (Fig. 7(d)), the *DW*s disappeared because the magnetic domains were fully magnetized parallel to the applied field. Figures 7(e) and (f) were obtained by tilting the specimen reversely. With the decrease of tilting angle, domain walls reappeared due to the reversed domains formed.

Changes in magnetic domains applying with the out-of-plane fields were observed in Fig. 8. Figure 8(a) was observed under the objective lens off, where the residual field was estimated to be about 150 Oe. The *DW*s continuously changed with the increase in applied filed and finally disappeared at 1480 Oe as shown in Fig. 8(e). In order to fully magnetize the domains along the applied field direction, huge magnetic field (1480 Oe) applied perpendicular to the film plane was needed compared to the in-plane field (37 Oe). *DW*s in right region as shown in Fig. 8(c) seemed to be not disappeared compared to the *DW*s in left; that is, magnetization rotation was retarded. It is noted that the TEM specimen thickness (t_s) between two regions is different each other. In order to confirm its thickness clearly, we obtained thickness map corresponding to a white rectangular region in Fig. 8(e) by EELS. The ratio of t_s to the mean free path for inelastic scattering (λ) is followed

$$t_s/\lambda = \ln(I_t/I_o)\,, \tag{2}$$

where I_t and I_0 are the total intensity and zero-loss

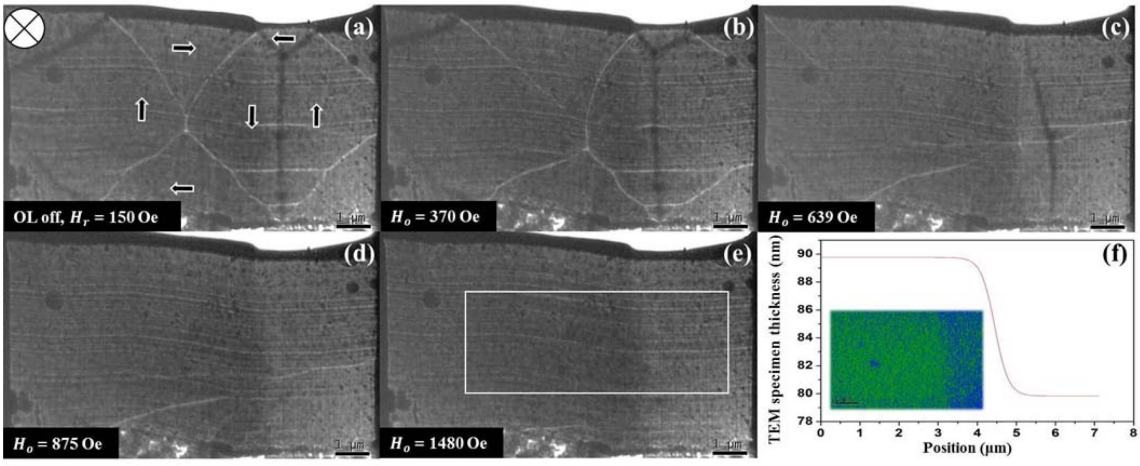

Fig. 8. (Color online) (a)-(e) Lorentz microscope images of Ni80-Fe20 thin film with applied the magnetic field to the out-of-plane. Black arrows, white circle and OL indicate the magnetization direction, applied field direction and objective lens respectively. (f) TEM specimen thickness (t_s) as a function of specimen position.

intensity in the EELS, respectively. The t_s (λ = 85 nm for permalloy film) as a function of specimen position are shown in Fig. 8(f) [24]. The thickness variation between two regions was measured as Δt_s = 10 nm, *i.e.*, 89 and 79 nm. It is reasonable to think that the magnetization direction at relatively thinner region is difficult to be rotated perpendicularly to the film

4. Conclusions

We analyzed the results obtained by the *in-situ* observation of magnetic domain wall motion in an electroplated Ni80-Fe20 thin film by Lorentz microscopy coupled with DPC microscopy. The H_c and B_s of electroplated Ni80-Fe20 thin film were 6.5 Oe and 1.56 T, attributed to nanocrystalline nature where the grain sizes (g) of 29 nm and sample thickness (t) of 3 μm were measured. The theoretical and measured values of domain width were 2.6 and 1.9 um, respectively. From the DPC images, we found the fluctuations of magnetization direction like zigzag pattern, attributed to two vortices with anticlockwise magnetization and its microstructures, *i.e.*, nanocrystallinity. Domain wall motions with the in-plane and out-of-plane fields applied were *in-situ* observed where the magnetization reversal was difficult in the out-of-field. For example in-plane field (37 Oe) and out-of-plane field (1480 Oe) were necessary to be fully magnetized to each field direction.

Acknowledgements

This research was supported by Basic Science Research Program through the National Research Foundation of Korea (NRF-2016R1D1A1B03934213) funded by the Ministry of Education.

References

[1] E. S. Machlin, Materials Science in Microelectronics II, Elsevier, New York (2010) pp. 57-64.
[2] T. Osaka, M. Takai, K. Hayashi, K. Ohashi, M. Saito, and K. Yamada, Nature **392**, 796 (1998).
[3] H. Q. Li and F. Ebrahimi, Acta Mater. **51**, 3905 (2003).
[4] T. Kasahara, H. S. Park, D. Shindo, H. Toshikawa, T. Sato, and K. Kondo, J. Magn. Magn. Mater. **305**, 165 (2006).
[5] M. C. Wurz, D. Dinulovic, and H. H. Gatzen, Meet. Electrochem. Soc. **206**, meeting abstract (2004).
[6] H. Seo, K. Nam, and K. Hong, J. Korean Magn. Soc. **22**, 42 (2012).
[7] H. J. Kim, J. Korean Magn. Soc. **21**, 77 (2011).
[8] H. Lee, W. Bang, K. Hong, Y.-D. Ko, J.-S. Chung, and H. Lee, J. Korean Magn. Soc. **19**, 138 (2009).
[9] X. D. Fan, A. B. Ma, H. Meb, G. Q. Xie, B. L. Shen, A. Makino, and A. Inoue, J. Appl. Phys. **109**, 07A314 (2011).
[10] H. S. Nalwa, Magnetic Nanostructures, American Scientific Publisher, Los Angeles (2002) pp 327-330.
[11] G. Herzer, IEEE Trans. Magn. **26**, 1397 (1990).
[12] H. S. Kim, S. Y. Jeong, C. H. Lee, and S. J. Suh, J. Kor. Magn. Soc. **21**, 193 (2011).
[13] H. S. Park, J. S. Baskin, and A. H. Zewail, Nano Lett. **10**, 3796 (2010).
[14] D. McGrouther, M.-J. Benitez, S. McFadzean, and S. McVitie, JEOL News **49**, 2 (2014).
[15] D. shindo, Analytical Electron Microscopy for Materials Science, Springer-Verlag, Tokyo (2002) pp. 109-116.
[16] R. Boll, Weichmagnetische Werkstoffe, Vacuumschmelze GmbH, Siemens AG Verlag, Berlin (1990).
[17] Vacuumschmelze GmbH Toroidal Cores of VITROPERM, data sheet PW-014 (1993).
[18] J. B. Yi, X. P. Li, J. Ding, and H. L. Seet, J. Alloys Compd. **428**, 230 (2007).
[19] K. Ishizuka and B. Allman, Microscopy Today **5**, 22 (2005).
[20] V. V. Volkov and Y. Zhu, Ultramicroscopy **98**, 271 (2004).
[21] K. Saito, H. S. Park, D. Shindo, and T. Yoshizawa, J. Magn. Magn. Mater. **305**, 304 (2006).
[22] T. Trunk, M. Redjdal, A. Kákay, M. F. Ruane, and F. B. Humphrey, J. Appl. Phys. **89**, 7606 (2001).
[23] C. M. Fu, P. C. Kao, M. S. Tsai, H. S. Hsu, C. C. Yu, and J. C. A. Huang, J. Magn. Magn. Mater. **239**, 17 (2002).
[24] Moorthy, S. K. E., Viret M. Rousseauo, and M. Kociak, Nano Lett. **12**, 2732 (2012).